ENGINEERING TRIPOS PART IB

Tuesday 2 June 1998 9.00 to 11.00

Paper 3

MATERIALS SOLUTIONS **FINAL VERSION**

1 (a) Need objective and constraint equations for stiffness performance index:

Objective in each case is to minimise mass: $m = \pi r^2 L \rho$ (i)

Stiffness Constraint is deflection; $\delta = \frac{F L^3}{3 E I}$ (ii)

Also $I = \frac{\pi r^4}{4}$ (iii)

Substitute (iii) in (ii) and rearrange $r = \left(\frac{4 F L^3}{3 E \pi \delta} \right)^{\frac{1}{4}}$

Eliminate free variable (r) in (i) $m = \sqrt{\frac{4 \pi F L^5}{3 \delta}} \times \frac{\rho}{\sqrt{E}}$

Hence *maximise* M1 for minimum mass $\underline{M1 = \frac{E^{1/2}}{\rho}}$

From data given (F, L and δ); Mass (M1) $\approx 131 \times \frac{\rho}{E^{1/2}}$ (1)

(b) Objective and constraint equations for strength performance index;

Strength Constraint is yield strength; $\sigma = \frac{F L r}{I}$ (iv)

Substitute (iii) in (iv) and rearrange $r = \left(\frac{4 F L}{\pi \sigma} \right)^{\frac{1}{3}}$

Eliminate free variable (r) in (i) $m = \left(4 \sqrt{\pi} F L^{\frac{5}{2}} \right)^{2/3} \times \frac{\rho}{\sigma^{2/3}}$

Hence *maximise* M2 for minimum mass $\underline{M2 = \frac{\sigma^{2/3}}{\rho}}$

From data given (F, L and δ); Mass (M2) $\approx 127 \times \frac{\rho}{\sigma^{2/3}}$ (2)

(c) Evaluation of M1 and M2 for the materials listed identifies CFRP clearly as the most suitable material on strength/stiffness criteria.

Material	Density, ρ (Mg m^{-3})	σf (MPa)	E (GPa)	*M1*	*M2*
Nylon	1.1	80	4	57	169
CFRP	1.6	1000	100	**198**	**625**
Aluminium Alloy	2.7	600	70	98	263

Mass per leg of fork can be calculated from equations (1) and (2) for each performance index as follows;

Material	Mass *(M1)* (kg per leg)	Mass *(M2)* (kg per leg)
Nylon	2.3	0.75
CFRP	**0.7**	0.20
Aluminium Alloy	1.3	0.48

The minimum mass of forks made from CFRP is given by the higher of the two values calculated above, i.e.; 0.7 kg per leg (≈ **1.4 kg per fork**). Note that the forks would not be stiff enough under the maximum working load if the lower value (0.2 kg per leg, 0.4 kg per fork) were selected.

(d) Other factors that influence the choice of material for the fabrication of bicycle forks include;

(i) Cost. This effectively eliminates CFRP (except for high performance racing machines). Reason why Ti alloys and steels are used commonly for this application.

(ii) Toughness. This determines whether the forks will fail under impact. Again eliminates CFRP.

(iii) Formability. Need to be able to form materials into sections (tubes rather than solid cylinders are used in practical fork design). Metals, again, have advantages here.

(iv) Manufacturability. Need to be able to manufacture components relatively easily. Eliminates hard and or brittle materials which require significant energy or thermal treatment to fabricate component parts. CFRP, for example, is difficult to shape.

(v) Solid cylinder model of forks not most appropriate (hollow cylinder better).

2 (a) Hardness of plain carbon steels is determined primarily by (i) carbon content (i.e. alloying) and (ii) microstructure (secondary phase formation). Good candidates may sketch increase in hardness or σ_y (and decrease in K_{1C} or ductility) with increasing carbon content. [Full marks for identifying factors (i) and (ii) with *brief* supporting discussion. The following gives more detail than required.]

Phase formation is determined primarily by solid state diffusion (thermally activated) of carbon atoms and undercooling in plain carbon steels. Practical processing is based on quench-hold processes with the hold temperature determining diffusivity and hence the phase composition of the steel. Plain carbon steels processed at different temperatures contain different amounts of cementite (Fe3C) which is a hard strong phase due to its high carbon content. The concentration and distribution of cementite, therefore, determines the hardness of the steel. Decreasing hold temperature of plain carbon steels (from the high temperature, 723°C, austenite phase) generally yields a finer distribution of cementite. Coarse pearlite (eutectoid ferrite and cementite), fine pearlite, upper bainite and lower bainite, for example, are produced by decreasing hold temperature.

Some carbon is retained by the ferrite lattice in the form of a solid solution for steels quenched from the austenite phase to room temperature. Martensite, for example, which consists entirely of a single iron phase with carbon in solid solution, is the hardest plain carbon steel. Hardness in this case is due mainly to effect of carbon atoms (solid solution hardening), rather than microstructure.

(b) Microstructure (i) is ~50%/50% ferrite and pearlite which contains typically 0.4 wt % C, (iii) is eutectoid pearlite containing 0.8 wt. % C, hence (ii) is martensite containing 0.8 wt. % C and (iv) is ferrite containing< 0.01wt. % C. Martensite is the hardest due to solid solution hardening. The hardness of the other microstructures decreases with decreasing cementite content (i.e. carbon content). Order in decreasing hardness, therefore, is (ii), (iii), (i), (iv).

(c) TTT curves (time-temperature-transformation) are used to relate the time and temperature of a phase transformation to the extent to which it occurs under isothermal processing conditions (i.e. constant temperature). There are a family of TTT curves for any transformation with each curve corresponding to a constant fraction of material transformed (i.e. from start, 1%, to finish, 100%). Undercooling below the equilibrium transformation temperature, T_E, provides the Gibbs free energy required to drive the

transformation. This determines the resulting phase distribution in the fully processed steel. [Credit given for schematic sketch of TTT curve.]

[The following is more detailed than required. Full marks for identifying around half the points made below for each microstructure. Half marks if only annotated TTT curves are given.]

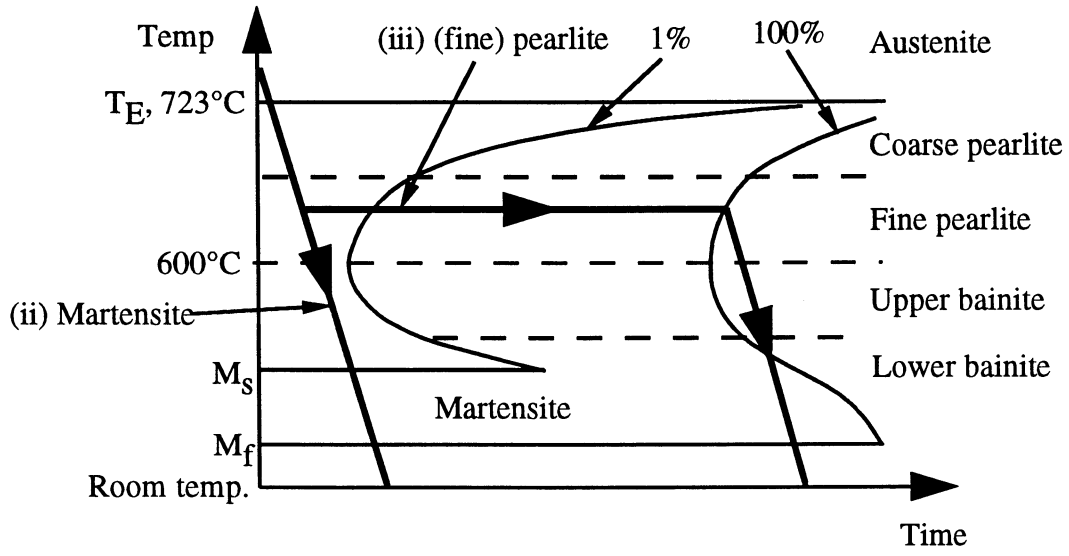

Microstructure (ii) (martensite) is single phase material formed by rapid cooling of austenite to "beat the nose" of the TTT curve and form a predominantly single phase material. Martensite consists of BCT (body centred tetragonal - α' phase) iron with up to 0.8 wt % carbon in solid solution (responsible for deformation of BCC lattice). The resultant microstructure consists of small grains which nucleate uniformly throughout the material. The fraction of martensite depends only on the temperature cooled rapidly to, not on time. Microstructure will contain 0% martensite at $T = M_S$ and 100% martensite at $T = M_f$ (the remaining phase will be retained as austenite of transform to bainite, depending on the hold time between M_S and M_f). Tempering of martensite is a separate process.

Microstructure (iii) (eutectoid pearlite) is two phase material formed by cooling the austenite phase and holding austenite at elevated temperature (i.e. between ~ 700°C < T_h < 600°C). Cementite (Fe_3C) precipitates out to form a Fe_3C - ferrite composite. Phase formation is controlled by diffusion. Hence it is kinetically favourable for the microstructure to form in alternate cementite/ferrite layers (minimises diffusion lengths for carbon atoms). Coarse pearlite forms at higher hold temperatures (~700°C) due to

increased diffusion rates. Fine pearlite forms at lower hold temperatures (~600°C). The hardness of pearlite is due mainly to the properties of the α-Fe3C phase boundary The harder cementite phase resists deformation of the softer ferrite phase. Hence, fine pearlite is harder than coarse pearlite due to the presence of more phase boundaries. Coarse pearlite, however, is more ductile.

(d) Fine eutectoid pearlite or tempered martensite give a good trade off between yield strength (~500MPa) and toughness (~50MPam$^{1/2}$) and either can be used for railway track (brief description of *either* required here). Fine eutectoid pearlite is harder than lower carbon content steel due mainly to the increased cementite content of the material (cementite is much more brittle than ferrite). Also the cementite - ferrite boundary is strong and the rigid cementite lattice restricts deformation of softer ferrite phase. Tempered martensite consists of extremely small and finely dispersed cementite particles embedded within a continuous ferrite matrix. Cementite - ferrite boundaries act as a barrier to dislocation movement and reinforces the ferrite matrix.

3 (a) The key features of the lead - tin phase diagram are:

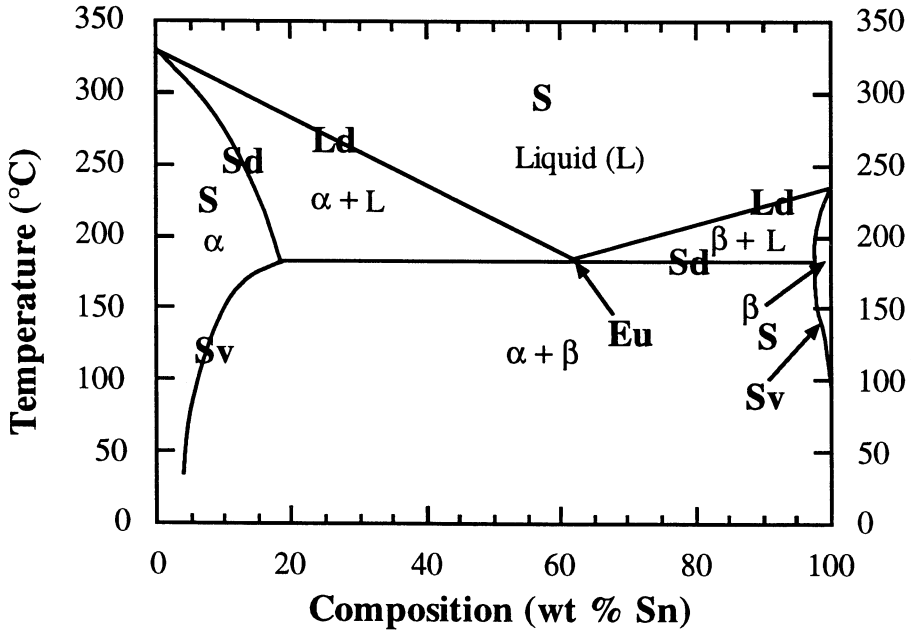

S; single phase, **Sd**; solidus, **Ld**; liquidus, **Sv**; solvus, **Eu**; eutectic point

(i) Three single phase regions; α, β and liquid. The α phase is a solid solution rich in Pb with Sn as the solute. The β phase is a solid solution rich in Sn with Pb as the solute.
(ii) Solidus lines are phase boundaries which define the top of a 100% solid field and separate solid and solid + liquid (α / α + L and β / β + L) regions of the phase diagram.
(iii) Liquidus lines are phase boundaries which define the bottom of a 100% liquid field and separate liquid and liquid + solid (L / α + L and L / β + L) regions of the phase diagram. (iv) Solvus lines separate single and two phase solid regions of the phase diagram (e.g. α / α + β phases).
(v) The eutectic point represents the lower limit of the single-phase liquid field formed by the intersection of the two liquidus lines and occurs at 60 wt % Sn and 183°C in this system. The liquid is transformed reversibly into two solid phases (α and β) at the eutectic temperature (i.e. the lowest temperature at which 100% liquid is stable) and composition. [2 marks for identifying features without explanation.]

(b) The quantity C_α is the composition at the α end of the phase field and C_β is the composition at the β end of the phase field at 150°C.
Derivation of the lever rule is based on two conservation of mass expressions;
1. The sum of the mass fractions of the two phases in a two phase alloy must sum to unity;

$$W_\alpha + W_\beta = 1$$

where W_α and W_β are the mass fractions of each phase (α and β in this example).
2. The mass of one of the components that is present in both phases must be equal to the mass of that component in the total alloy;

$$W_\alpha C_\alpha + W_\beta C_\beta = C_0$$

where C_0 is the overall composition of that component in the alloy.

Solution of these simultaneous equations yields;

$$W_\alpha = \frac{C_0 - C_\beta}{C_\alpha - C_\beta} \qquad \text{and} \qquad W_\beta = \frac{C_\alpha - C_0}{C_\alpha - C_\beta}$$

For the α phase fraction in an α + β phase field, therefore, $W_\alpha = \frac{C_0 - C_\beta}{C_\alpha - C_\beta}$.

This is the lever rule for calculating the mass fraction of one particular phase in a two phase alloy of known net composition at a given temperature and is used as follows;

1. Tie line is constructed across the two-phase region at the temperature of the alloy.
2. The overall alloy composition is located on the tie line.
3. The fraction of the phase at one end of the tie line is calculated by taking the length of the tie line from the overall alloy composition to the phase at the other end of the tie line and dividing by the total length of the tie line.

(c) Phases and compositions for a 40 wt % Sn and 60 wt % Pb alloy at 150°C;

Plot this composition/temperature point on the phase diagram (shown below as B). Shows that α and β phases co-exist. Composition of each phase determined by constructing tie line across the α + β phase field at 150°C as shown below. The composition of the α phase corresponds to the tie line intersection with the α/(α+β) solvus phase boundary - about 10 wt % Sn and 90 wt % Pb (denoted as C_α).

Similarly the β phase has composition approximately 97 wt % Sn and 3 wt % Pb from Fig. 3. [Fig. 4.2 in the Data Book yields a lower Sn-content B phase alloy].

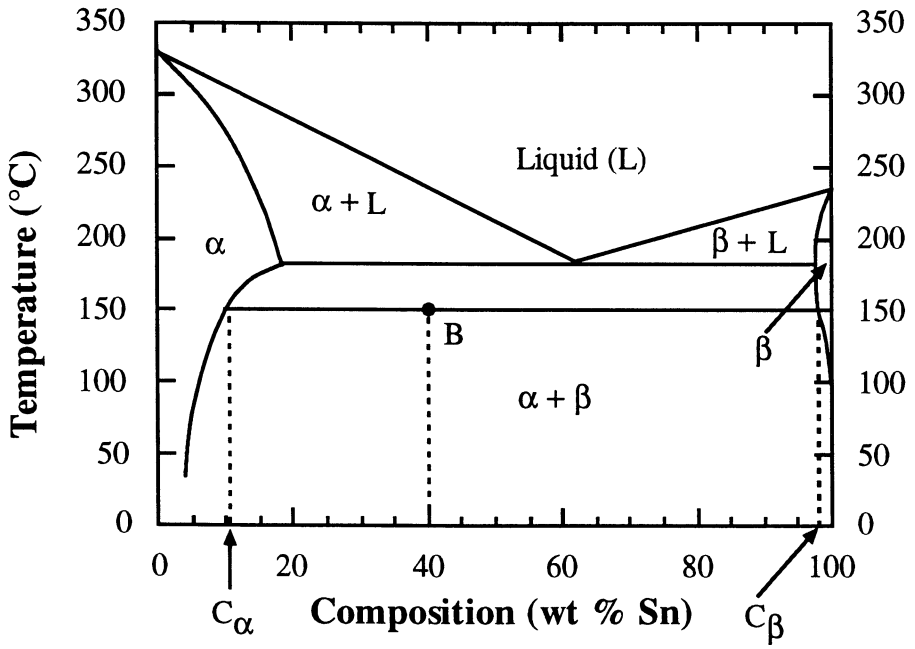

It is necessary to employ the lever rule to determine the relative amount of each phase present in the 40 wt % Sn and 60 wt % Pb alloy in terms of its mass fraction since the

alloy consists of two phases. The mass fractions W_α and W_β can be calculated as follows;

$$W_\alpha = \frac{C_\beta - C_0}{C_\beta - C_\alpha} = \frac{98 - 40}{98 - 10} = \mathbf{0.66\ wt\ \%}$$

$$W_\beta = \frac{C_0 - C_\alpha}{C_\beta - C_\alpha} = \frac{40 - 10}{98 - 10} = \mathbf{0.34\ wt\ \%}$$

where C_0 is the overall alloy composition.

(d) Solder has a composition of 60 wt % Sn and 40 wt % Pb. This is the eutectic composition for this system which has the lowest possible melting point ($\approx$ 185°C) for a Sn-Pb alloy. This alloy is particularly suitable for joining applications since it is easily melted and for electronic applications where it is desirable to minimise the heat input into individual devices.

4. (a) The terms wrought and cast relate to the *shaping properties* of aluminium alloy.

Wrought: A material that is suitable for shaping by a working process, e.g. forging, rolling, extrusion. Applies to a wide range of alloy compositions within a phase system. Usually heat-treatable.
Cast: A material that is suitable for shaping by a casting process. Applies to alloys close to eutectic composition to achieve the necessary liquid "flow". Usually non heat-treatable.

(b) Aluminium alloys precipitation harden with heat treatment. This is achieved by two different heat treatments. Heating composition C_0 in a binary ($\alpha + \beta$) phase system above the $\alpha/(\alpha + \beta)$ solvus line to T_0 causes the β phase to dissolve (maximum solubility at M) to form a single phase (α). Rapid cooling or quenching to T_1 (i.e. to within the ($\alpha + \beta$) phase region - typically room temperature) yields a non-equilibrium α phase. This supersaturated material is unstable and relatively soft. Such a material will age harden as the β phase precipitates out slowly over time at room temperature. This thermally activated process can be accelerated significantly by heating the supersaturated α solid solution to a higher temperature T_2 within the ($\alpha + \beta$) phase region (i.e. below the $\alpha/(\alpha + \beta)$ solvus) at which the solid state diffusion rates become appreciable. The β phase begins to precipitate out of the α solid solution more rapidly at this temperature in the form of

finely dispersed particles of composition C_β to significantly increase the hardness and yield strength of the material. This process is termed ageing (see ageing curve). Hardness and yield strength decrease if the precipitant particles become too large due to their reduced effectiveness in pinning dislocations. This is termed overageing. Overageing can be reversed by heating the alloy above the $\alpha/(\alpha + \beta)$ solvus line to re-dissolve the β phase and the second heat treatment repeated.

Other factors associated with the heat treatment process that may account for an increase in hardness in Al alloys are; (i) coherency strains around the Guinier-Preston (GP) zones generate stresses that help prevent dislocation movement; (ii) the microstructure of the GP precipitant phase influences the mechanism by which dislocations move through the material; (iii) GP phase boundaries inhibit the motion of dislocations. All these points are creditworthy.

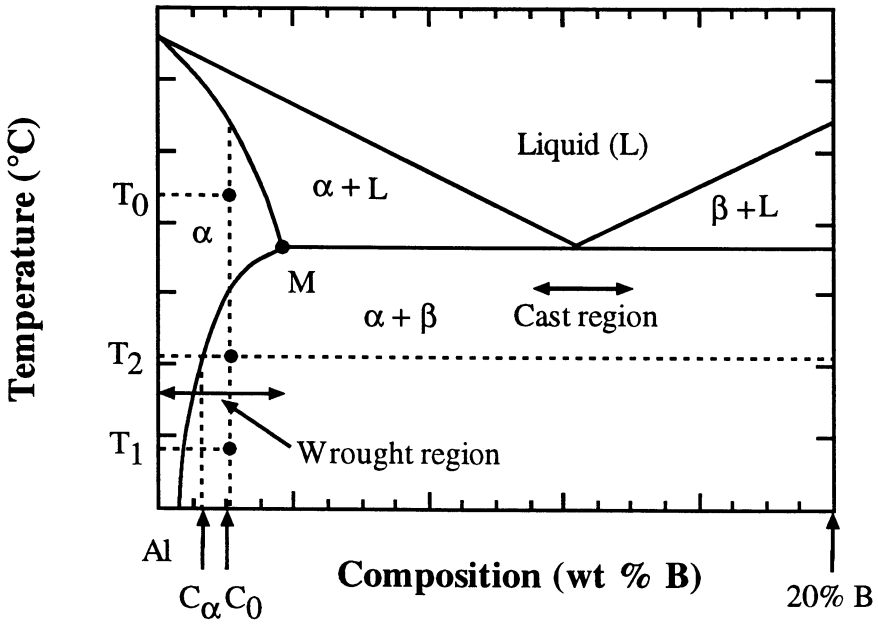

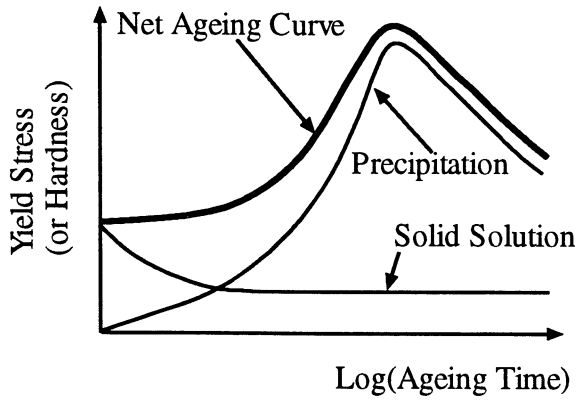

(c) Full marks for a solution which explains; (i) the difference between heat treatable and non heat treatable wrought alloys; (ii) the eutectic nature of cast alloys which generally inhibits the formation of precipitates and hence hardening; (iii) 2 examples.

Cast aluminium alloys must necessarily lie close to the eutectic composition to achieve the required fluidity properties. This invariably yields a coarse eutectic, layered structure on quenching which is not generally suitable for precipitate hardening. The α part of eutectic composition cast alloys can age harden, however, by partial solution treatment below the eutectic temperature although this is not a particularly rapid process.

Wrought aluminium alloys are formed from a much wider stable two phase field at the Al end of the phase diagram (see diagram above) and are therefore much more suitable for precipitate hardening. In general wrought alloy compositions containing a wt % of alloy phase lying in the α phase field at room temperature, however, contain only a solid solution of the α phase an hence cannot be precipitate hardened. In addition, some alloys such as Al and 5 wt % Mg prepared by rapid cooling from the α phase region cross the two phase boundary (solvus) but won't precipitate since the cooling rate misses the nose of the C curve. In this case a barrier exists against nucleation, despite the presence of a supersaturated solution. Hardening in these and in single phase field materials is limited to solution and work hardening. These materials do not age harden.

Examples (page 31 of Data Book!)

	Wrought	Cast
Heat Treatable	Al-Cu (4 wt %)	Al-Si(5)-Mg(0.6)
	Al-Cu(0.4)-Mg/Si/Mn (<1%)	
	Al-Zn(6)-Mg(3)-Cu,Mn(<1%)	
Non Heat Treatable	Al-Mn (1.25 wt %)	Al-Si (12 wt %)
	Al-Mg (7 wt %)	Al-Si(5)-Cu(3)

(d) Again, see page 31 of Data Book.
(i) 2000 series aluminium alloy [e.g. Al-Cu(4.4%)-Mg(0.5%)] rivets precipitation harden at room temperature after quenching which decreases their ductility and makes them too hard. Refrigeration reduces the solid state diffusion rates and hence the degree of precipitate hardening.

(ii) 5000 series aluminium alloys [e.g. Al-Fe(0.7%)-Mg(1.5%)] are strengthened by cold working, not heat treatment. Welding, therefore, will recrystallise the solid phase, annealing out any dislocations in heat affected zone (HAZ). This can weaken the structure significantly.

5 (a) For a test specimen under tensile stress: $P_s(V_0) = \exp\left\{-\left(\frac{\sigma}{\sigma_0}\right)^m\right\}$

Hence the probability of survival = 1/e = 0.37 when the applied stress, σ, is equal to reference strength σ_0 for a batch of identical samples of volume V_0. This parameter, therefore, is simply the tensile stress under which 37% of the test samples survive. The Weibull modulus m describes how rapidly the strength of the material falls as $\sigma \rightarrow \sigma_0$. The lower m, the greater the variability of strength of material. The larger the m the more homogeneous the material. In practice m varies between 5 and 20 for most brittle materials.

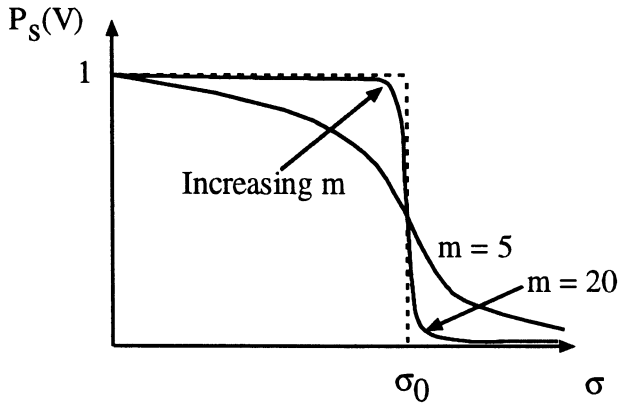

m and σ_0 are measured in laboratory tests on specimens of identical geometry. Each specimen is tested to failure under an applied tensile or bending load, σ_f. The probability of survival P_S for each test piece is then calculated relative to the other samples in the distribution. ln (ln $1/P_S$) is then plotted against ln (σ_f) to form a straight line graph. The gradient of the graph gives m and the intercept with the ordinate axis σ_0. If ordinate axis is labelled with P_S, σ_0 is simply read off at 37%.

(b) The probability of failure of a test specimen varies with the mode of loading (generally tensile or bending) due to a variation in stress within the test piece. A specimen tested in tension, for example, experiences a constant tensile stress over its entire cross section

whereas the same specimen in bending only experiences tensile forces on one side of the neutral axis. In this case flaws in the side of the specimen under compression do not influence the breaking load (ceramics are ~ 10 times stronger in compression than tension). In addition, the tensile stress of a sample under bending varies with distance from the neutral axis, increasing from zero to a maximum at the top surface of the sample. Thus the average stress in the material decreases and the test specimen can withstand higher applied loads before breaking. As a result a ceramic specimen is stronger in bending than in simple tension. The variation in stress in the sample under bending is taken into account by integrating the stress over the sample volume (trivial for a specimen under tension). [N.B. stress varies with both width and length for specimens under 3-point bend test].

(c) $$P_s(V) = \exp\left\{ -\frac{1}{\sigma_0^m V_0} \int_V \sigma^m \, dV \right\} \qquad \text{hence, } -\ln(P_s) = \frac{1}{\sigma_0^m V_0} \int_V \sigma^m \, dV$$

For a test specimen of rectangular cross section under 4-point loading, the tensile stress increases linearly from the neutral axis to the upper surface of the sample but does not vary with distance along the length of the test rod (constant radius of curvature). Tensile stress is maximum at the centre of the upper surface of the specimen.

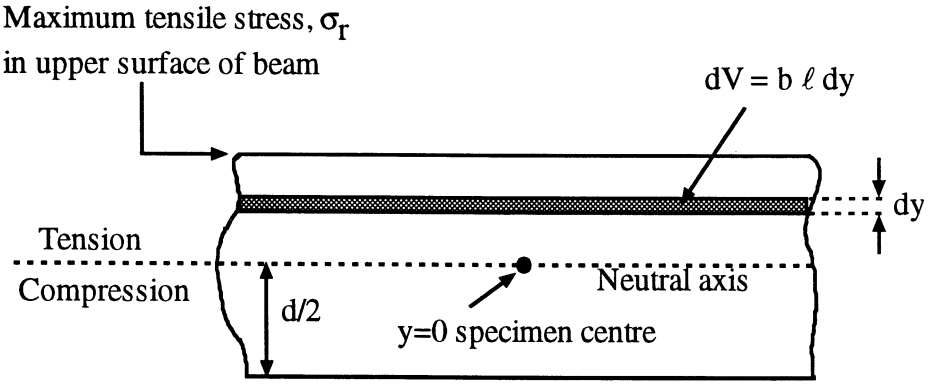

For the specimen in pure bending;

$$dV = b\,\ell\,dy, \quad \text{therefore} \qquad -\ln(P_s) = \frac{1}{\sigma_0^m V_0} \int_V \sigma^m \, b\,\ell\,dy$$

Integrate over $\int_0^{d/2} dy$ since only half of beam in tension (y = 0 to $\ell/2$).

write $\sigma(y) = \sigma_r \frac{y}{d/2}$ $\qquad \int_V \sigma^m dV = b\ell \int_0^{d/2} \left(\sigma_r \frac{y}{d/2}\right)^m dy$

$$\int_V \sigma^m dV = b\ell\sigma_r^m \frac{2^m}{d^m}\left[\frac{y^{m+1}}{m+1}\right]_0^{d/2} = b\ell\sigma_r^m \frac{2^m d^{m+1}}{d^m 2^{m+1}(m+1)} = \frac{b\ell d\sigma_r^m}{2(m+1)}$$

Hence for the beam under 4-point test; $\qquad -\ln P_s = \left(\frac{\sigma_r}{\sigma_0}\right)^m \frac{b\ell d}{V_0 2(m+1)}$ $\qquad$ (1)

For the beam under uniform tension; $\qquad -\ln(P_s) = \frac{b d \ell}{V_0}\left(\frac{\sigma_t}{\sigma_0}\right)^m$ $\qquad$ (2)

Determine relative strengths of the specimens under the different load conditions for the same probability of failure. Hence, equating (1) and (2);

$$\frac{\sigma_r^m b\ell d}{2(m+1)} = \sigma_t^m b d \ell$$

$$\frac{\sigma_r}{\sigma_t} = 2^{1/m}(m+1)^{1/m} \qquad \text{QED}$$

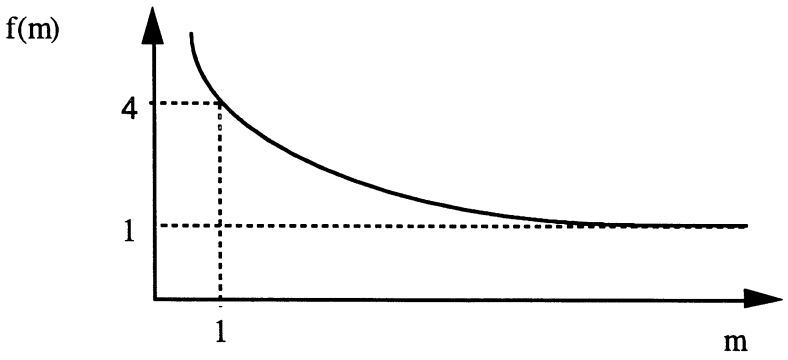

(d) Probability of failure = 50% in bend test for an applied maximum stress (i.e. at the upper surface of the specimen) of 214 MPa. An applied stress of 214 MPa in a bend test, therefore, corresponds to a strength of $\frac{214\ \text{MPa}}{[2(m+1)]^{1/m}} = 130$ MPa in an axial tensile test.

In axial test: $P_s(V) = \exp\left\{-\frac{V}{V_0}\left(\frac{\sigma}{\sigma_0}\right)^m\right\}$

Test specimens $V_1 = 5 \times 5 \times 20 = 500\ mm^3$, $\sigma_1 = 130$ MPa, $m = 5$, $P_{s1} = 0.5$

Service specimens $V_2 = 10 \times 10 \times 50 = 5000\ mm^3$, $\sigma_2 = 30$ MPa, $m = 5$, $P_{s2} = ?$

$$-\ln P_s = -\frac{V}{V_0}\left(\frac{\sigma}{\sigma_0}\right)^m \qquad \text{therefore} \qquad \frac{\ln P_{s2}}{\ln P_{s1}} = \frac{V_2\,\sigma_2^m}{V_1\,\sigma_1^m}$$

$$\ln P_{s2} = \ln 0.5 \times \frac{V_2}{V_1} \times \frac{\sigma_2^m}{\sigma_1^m} = \ln 0.5 \times 10 \times \left(\frac{30}{130}\right)^5 \qquad \ln P_{s2} = -0.00454$$

i.e. $\mathbf{P_{s2} \sim 0.995}$ (specimen rejection rate of 0.5%).

6. (a) Thermoplastics soften on heating. Secondary forces between long chain polymer molecules melt (thermal energy exceeds bond energy) which causes an increase in the mobility of molecules and hence a change in the properties of the polymer at the so-called glass transition temperature. Degree to which properties vary depends significantly on crystallinity of thermoplastic.

Thermoplastics exhibit pronounced change in elastic modulus above and below T_g.
Above T_g; Soft, rubbery, reasonably tough, behaves like a viscous liquid and creeps significantly.
Below T_g; Harder, brittle, glassy state. Toughness falls steeply as temperature is reduced. Time and creep behaviour becomes less marked due to increased stiffness of secondary bonded long polymer molecules. Failure below T_g is by drawing (deformation) or crazing at lower temperature.
Vicinity of T_g; Creep behaviour becomes pronounced c.f. lower temperature state with thermoplastic exhibiting combined mechanical properties of high and low temperature extremes. i.e. it behaves viscoelastically. Mechanical behaviour often termed "leathery"" at temperature ~ T_g.
Young's modulus varies with temperature as follows;

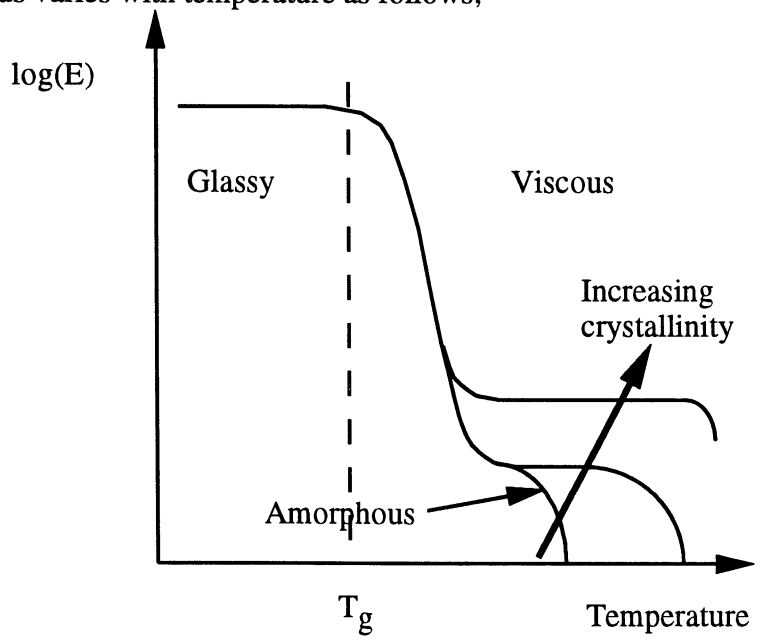

Modulus falls typically by a factor of up to 500 at T_g and occurs at a temperature of between 0.5 and 0.8 T_m. Depends on degree of crystallinity of polymer, however.

(b) The spring describes the elastic behaviour (lower temperature) of the polymer whereas the dashpot account for its viscous (higher temperature) behaviour. The series combination of E and η gives rise to an instantaneous extension of the polymer (due to the spring) followed by creep with time (dashpot). Partial recovery is obtained on removal of the load as the spring relaxes (no relaxation of the dashpot occurs and the polymer remains deformed permanently). The displacements of the spring and dashpot in the arrangement, therefore, are generally not equal.

On initial application of a force to the arrangement in Fig. 5, element E strains elastically, corresponding to instantaneous deformation of the polymer. Further strain of the arrangement (deformation creep) then occurs as a decaying function of time and is determined by the properties of the dashpot. Element E relaxes instantly on removal of the stress which corresponds to partial instantaneous recovery. The polymer is thus left in a permanently deformed state.

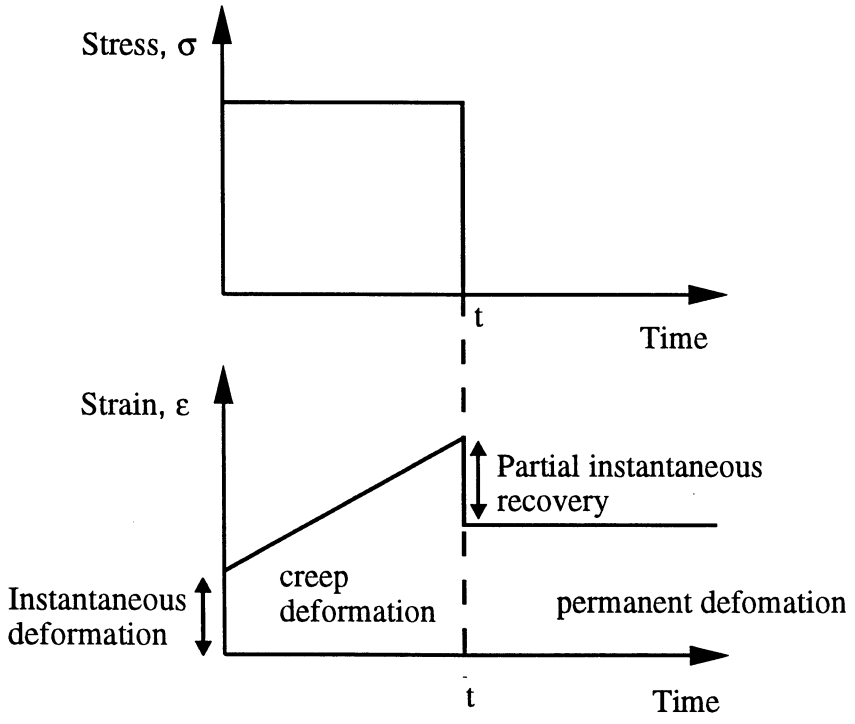

(c) Strain rate of dashpot ;

$$\dot{\varepsilon}_{dashpot} = \frac{\sigma}{\eta} \quad \text{therefore, } \varepsilon_{dashpot} = \frac{\sigma t}{\eta} \quad \text{for constant stress.}$$

Strain of spring

$$\varepsilon_{spring} = \frac{\sigma}{E_1}$$

Hence strain generated by the spring/dashpot arrangement;

$$\varepsilon_m(t) = \frac{\sigma}{E_1} + \frac{\sigma t}{\eta_1}$$

(d) Neglecting weight of polymer

At t = 0; $\varepsilon = \frac{8}{500} = \frac{500}{25 \times 10^{-6} E}$ i.e. E = 1.25 GPa

At t = 48 hours $\varepsilon = \frac{70}{500} = \frac{8}{500} + \frac{500 \times 48 \times 60 \times 60}{25 \times 10^{-6} \eta}$

i.e. η = 28 TPa.s

Use E to identify polymer. From Data Book candidates are

Thermosets;	epoxies (E = 0.5 to 2 MPa)
Thermoplastics;	polyesters (E = 1 to 5 MPa)

The subject of the test is clearly creeping, hence it is more likely to be a thermoplastic.
i.e. **Polyester**.